

Maximizing Revenue with Adaptive Modulation and Multiple FECs in Flexible Optical Networks

Cao Chen, Fen Zhou, *Senior Member, IEEE*, Massimo Tornatore, *Senior Member, IEEE*, Shilin Xiao

Abstract—Flexible optical networks (FONs) are being adopted to accommodate the increasingly heterogeneous traffic in today’s Internet. However, in presence of high traffic load, not all offered traffic can be satisfied at all time. As carried traffic load brings revenues to operators, traffic blocking due to limited spectrum resource leads to revenue losses. In this study, given a set of traffic requests to be provisioned, we consider the problem of maximizing operator’s revenue, subject to limited spectrum resource and physical layer impairments (PLIs), namely amplified spontaneous emission noise (ASE), self-channel interference (SCI), cross-channel interference (XCI), and node crosstalk. In FONs, adaptive modulation, multiple FEC, and the tuning of power spectrum density (PSD) can be effectively employed to mitigate the impact of PLIs. Hence, in our study, we propose a universal bandwidth-related impairment evaluation model based on channel bandwidth, which allows a performance analysis for different PSD, FEC and modulations. Leveraging this PLI model and a piecewise linear fitting function, we succeed to formulate the revenue maximization problem as a mixed integer linear program. Then, to solve the problem on larger network instances, a fast two-phase heuristic algorithm is also proposed, which is shown to be near-optimal for revenue maximization. Through simulations, we demonstrate that using adaptive modulation enables to significantly increase revenues in the scenario of high signal-to-noise ratio (SNR), where the revenue can even be doubled for high traffic load, while using multiple FECs is more profitable for scenarios with low SNR.

Index terms— Flexible optical networks (FONs); revenue maximization; adaptive modulation; multiple forward-error correction (FEC);

I. INTRODUCTION

According to recent traffic reports, network traffic (fueled by successful network services like video on demand, file sharing, online gaming, and video conferencing) is still growing exponentially in today’s Internet [2]. This constant traffic growth can be accommodated by novel flexible optical networks (FONs) which can support large transmission capacity. As busy hour traffic peaks are expected to increase almost 5

Cao Chen is with the State Key Laboratory of Advanced Optical Communication Systems and Networks, Shanghai Jiao Tong University, Shanghai, 200240, China (email: cao.chen@alumni.univ-avignon.fr). Cao Chen is also with the CERI-LIA in University of Avignon, France.

Fen Zhou is with the CERI-SN, IMT Lille Douai, Institut Mines-Télécom, University of Lille, Villeneuve-d’Ascq, 59650, France. He is also with the CERI-LIA, University of Avignon, France. (email: fen.zhou@imt-lille-douai.fr).

Massimo Tornatore is with the Department of Electronics, Information and Bioengineering in Politecnico di Milano, Italy (email: massimo.tornatore@polimi.it).

Shilin Xiao is with the State Key Laboratory of Advanced Optical Communication Systems and Networks, Shanghai Jiao Tong University, Shanghai, 200240, China (email: slxiao@sjtu.edu.cn).

A preliminary version of this work was presented as a short paper at IEEE HPCC 2019 [1].

times between 2017 and 2022 (average Internet traffic will increase only 3.7 times), the problem of coping with sudden resource crunches will become even more a matter of concern in next years, especially during peak usage periods [2]–[5]. During resource crunch, given the limited spectrum resources in FONs, not all traffic requests can be fully satisfied and some traffic must be blocked. As carried traffic brings revenue to operators, resource crunch events can lead to significant revenue losses for operators. Hence, efficient provisioning strategies in optical networks are required to reduce blocking and maximize operators’ revenue.

In FONs, an adequate amount of spectrum resources to establish a lightpath is required for each request. Since FONs can support variable routes, bandwidth, and modulation formats (MFs), the routing and wavelength assignment problem has evolved into the routing and spectrum assignment [6]–[9]. However, since the spectral efficiency granularity of m -ary quadrature amplitude modulation (m QAM) is coarse, the conventional resource provisioning cannot give full play to its advantages in collecting the services’ revenue. Hence, to achieve even higher resource-allocation flexibility that granted by multiple MFs, tunability of forward error-corrections has been introduced to adjust the spectral efficiency [10]–[13]. It can be typically observed that overhead ratios range values from 7% to 20%. The combination of MF and FEC, referred to as *transmission mode* in this paper, can provide more candidate choices in terms of spectral efficiency and transmission reach. Compared to the traditional approaches aiming at revenue improvement, such as using backup lightpaths for living traffic [14] or upgrading to multi-core fibers [15], using MF and FEC is more efficient and faster. The traffic provisioning with multiple MFs and FECs maps into a problem of routing, MF, FEC, and spectrum assignment (RMFSA) [16]. Although some researchers have proposed heuristic algorithms [9, 10, 13], like *congestion-aware sequential loading* algorithm [17], and *adaptive FEC selection* [18], there is no complete mathematical model for the lightpath provisioning in FONs with both MF and FEC, which also accounts for physical layer impairments (PLIs) modeling. While the optimal combination of MF and FEC has been investigated at the transmission layer in, *e.g.*, [19], in this paper we investigate how the combination of MF and FEC can be used to maximize revenues through appropriate traffic provisioning strategies.

To support multiple MFs and FECs in FONs, traffic provisioning strategies must be cross-layer [20], *i.e.*, they must be capable of taking in account physical layer aspects, to achieve efficient spectrum usage. The PLIs of a lightpath are influenced by the bandwidth, by power spectral densities (PSDs), by the route length, and by the number of crossed nodes.

Due to the impact of all the parameters just mentioned, the quality of transmission (QoT) (e.g., expressed by lightpath's Signal to Noise Ratio, SNR) may deteriorate and fall below acceptable threshold for correct signal reception after a long distance. Recent studies on the node crosstalk have considered the wavelength-related and frequency slot-related crosstalk component [21, 22]. However, current studies overestimate the PLIs with the assumption of full wavelength or full consecutive frequency slots for each lightpath. For example, the node crosstalk on provisioned bandwidth of 12.5 GHz slot is larger than the actual value of the sub-channel bandwidth with 6.25 GHz [23]–[25]. To reduce the PLIs, a guard band (e.g, 12.5 GHz) may be used, but incurring in inefficient usage of spectrum resources. Therefore, the PLI model that we propose is based on channel bandwidth, which means that the impairments of node crosstalk and fiber nonlinear interference are evaluated by the bandwidth rather than a wavelength or slot, which ensures that the PLIs are properly estimated and spectrum resource is effectively utilized.

The main novelty and contributions of this paper can be summarized as follows:

- 1) We devise novel traffic provisioning strategies to maximize the total revenue using different MF and FEC configurations. The lightpaths can adopt transmission mode with either higher spectral efficiency or longer transmission reach to guarantee the bit-rate under resource crunch. Compared to single MF or single FEC, the combination can provide just-enough spectral efficiency and transmission reach thus improve the traffic provisioning. By using a piece-wise linear fitting function to model the nonlinear interference and calculating the crosstalk of intermediate nodes, we linearize the PLIs then model the studied problem as a mixed integer linear program (MILP). Our MILP model is based on flow rather than pre-calculated route. Without using the candidate route, our method can get the optimal solution irrespective of the number of routes.
- 2) We propose a novel lightpath's PLI evaluation model based on the channel bandwidth that incorporates the impact of different PSDs, FECs, and MFs. By tracing the relationship between the PSD and SNR, we observe that using MFs enables to increase revenues with high SNR, while using multiple FECs is preferred for the scenarios of low SNR. Besides, compared to the wavelength-related or frequency slot-related method, the bandwidth-related method evaluates the PLIs by using channel bandwidth. To this end, the spectrum resources of fiber are assumed to be continuous rather than discrete frequency slot.
- 3) A fast and near-optimal heuristic algorithm is also proposed to solve the revenue maximization problem.

The rest of this paper is organized as follows. We describe our proposed PLI model in Sec. II. The problem of traffic provisioning with adaptive MFs and multiple FECs is stated in Sec. III. To solve it, we present a MILP model in Sec. IV and a heuristic algorithm in Sec. V. Illustrative numerical results are presented in Sec. VI. Finally, Sec. VII concludes this paper.

II. PHYSICAL LAYER MODEL

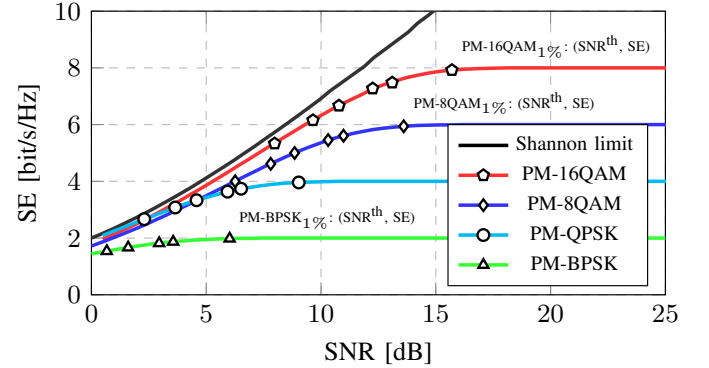
In this section, we discuss our proposed PLI evaluation model. We also include a description of the signal impairments and of the optical transmission.

A. MF and FEC

We denote as transmission mode \mathcal{C} the combination set of MF and FEC, $\mathcal{C} = (\mathcal{M}, \mathcal{F})$. For an arbitrary transmission mode $c \in \mathcal{C}$, its spectral efficiency is

$$SE(c) = SE(m, f) = m / (1 + OH_f) \quad (1)$$

where m is the theoretically maximum spectral efficiency of the MF, and OH_f is the FEC overhead ($\times 100\%$) [11, 19]. The spectral efficiency and SNR threshold of several transmission modes are shown in Fig. 1. In particular, we assume four available polarization-multiplexing MFs (PM-BPSK, PM-QPSK, PM-8QAM, and PM-16QAM) and six FEC OHs (1%, 7%, 10%, 20%, 30%, and 50%). For example, the spectral efficiency of PM-16QAM with FEC OHs 10% is $4/(1+10\%) = 3.63$ bit/s/Hz, while the SNR threshold is 15.7 dB. To satisfy QoT, the SNR should be over the threshold for each transmission mode. Next, we present the PLI model that impacts SNR.



MF	m	FEC					
		OH=1%	OH=7%	OH=10%	OH=20%	OH=30%	OH=50%
PM-BPSK	2	6.02	3.56	2.95	1.6	0.67	-
PM-QPSK	4	9.03	6.52	5.93	4.58	3.65	2.3
PM-8QAM	6	13.6	10.98	10.31	8.85	7.81	6.26
PM-16QAM	8	15.7	13.1	12.25	10.78	9.65	7.98

Fig. 1. The maximum achievable spectral efficiency of different transmission modes with different SNRs [11, 26]. With a target pre-FEC BER of 10^{-4} , the SNR threshold for each marker is illustrated in the table below.

B. PLIs model

When an optical signal propagates, it suffers diverse forms of PLIs, including white Gaussian noise amplified spontaneous emission (ASE), self-channel interference (SCI), and cross-channel interference (XCI) [8, 27, 28]. Both SCI and XCI interference are caused by the Kerr effect of fiber, which can be estimated as additive white Gaussian noise by the GN model [27]. When a signal traverses an optical cross-connect (OXC), the node crosstalk from signal adding or dropping (AD) at node must be also considered [20, 21].

The PLI related parameters are given in Table I. We note c_i as the transmission mode used by request i . SNR_i denotes its received signal-to-noise ratio, and $\text{SNR}_{c_i}^{\text{th}}$ is the SNR threshold for c_i . By summing up all noise contributions due to PLIs, a request i can be served if it satisfies the QoT constraint as in Eq. (2).

$$\text{SNR}_i = \frac{G_i}{G_i^{\text{ASE}} + G_i^{\text{SCI}} + G_i^{\text{XCI}} + G_i^{\text{AD}}} \geq \text{SNR}_{c_i}^{\text{th}} \quad (2)$$

For ease of the MILP modeling, we can also express Eq. (2) in its reciprocal form,

$$\left\{ \begin{array}{l} \frac{1}{\text{SNR}_i} = t_i^{\text{ASE}} + t_i^{\text{SCI}} + t_i^{\text{XCI}} + t_i^{\text{AD}} \leq \frac{1}{\text{SNR}_{c_i}^{\text{th}}} \\ t_i^{\text{ASE}} = G_i^{\text{ASE}}/G_i \\ t_i^{\text{SCI}} = G_i^{\text{SCI}}/G_i \\ t_i^{\text{XCI}} = G_i^{\text{XCI}}/G_i \\ t_i^{\text{AD}} = G_i^{\text{AD}}/G_i \end{array} \right. \quad (3)$$

where t_i^{ASE} , t_i^{SCI} , t_i^{XCI} , and t_i^{AD} are the noise to signal ratios of ASE, SCI, XCI, and AD node crosstalk, respectively. The noise to signal ratios can be regarded as the amount of PLIs of ASE, SCI, XCI, and node crosstalk. In the following, we will explain in detail the computation of various impairments.

TABLE I
PARAMETERS FOR PLIS

Parameters and description	
α	Power attenuation ratio of fiber, 0.2 dB/km.
β_2	Second order dispersion of 1550nm wavelength, -21.7 ps ² /km.
γ	Non-linear coefficient, 1.3 (W-Km) ⁻¹ .
h	Planck's constant.
ν	Frequency of optical signal, 192.5 THz.
μ	$\frac{3\gamma^2}{2\pi\alpha\beta_2}$.
ρ	$\pi^2\beta_2/\alpha$.
ϵ_X	OXC port leakage ratio, -25 dB.
n_{sp}	Noise factor of optical amplifier, 7dB.
G_i	Power spectral density of request i .
G_i^{ASE}	PSD of ASE.
G_i^{SCI}	PSD of SCI.
G_i^{XCI}	PSD of XCI.
G_{ijv}^{AD}	PSD of AD node crosstalk from j to i .
G_i^{AD}	PSD of AD, $G_i^{\text{AD}} = \sum_{jv} G_{ijv}^{\text{AD}}$.
SNR_c^{th}	SNR threshold of transmission mode c .
L_{span}	Span length, 100 km/span.

1) *Impairments along fibers (ASE, SCI, and XCI):* ASE noise is a white noise, whose intensity is proportional to the number of fiber spans and channel bandwidth. Its PSD can be expressed by

$$G_i^{\text{ASE}} = N_{\text{span}}(e^{\alpha L_{\text{span}}} - 1)n_{\text{sp}}h\nu \quad (4)$$

where N_{span} is the number of spans (see Table I for the other parameters).

In GN model [27], both SCI and XCI are regarded as white noise, whose PSD is related to the light power, bandwidth and center frequency. Eqs. (5) and (6) can be used to calculate the PSD of SCI and XCI [28, 29] (note that the calculation has been validated for bandwidth Δf_i bigger than 28 GHz [28].

$$G_i^{\text{SCI}} = N_{\text{span}}\mu G_i^3 \text{arcsinh}(\rho\Delta f_i^2) \quad (5)$$

$$G_i^{\text{XCI}} = \sum_j N_{\text{span},ij}\mu G_i G_j^2 \ln \left(\frac{|f_i - f_j| + \Delta f_j/2}{|f_i - f_j| - \Delta f_j/2} \right) \quad (6)$$

where Δf_i is the bandwidth of request i (unit: GHz), and f_i is the relative carrier center frequency (unit: GHz).

2) *Impairments at nodes :* Impairments at nodes come from filtering effects and node crosstalk. In-band crosstalk is considered in this paper, *i.e.* the lightpath experiences node crosstalk if it is exposed to the other lightpaths with the overlapping bandwidth. As an example, we use 9-node network in Fig. 2(a) to illustrate the different node crosstalk components. The primary signal P1 is added at node C1, passes through node C2, and is dropped at node C3. Other three crosstalk signals I1, I2, and I3, are also depicted. At each of its nodes(C1, C2 and C3), P1 will experience all forms of crosstalk, *i.e.* adding, passing through, and dropping.

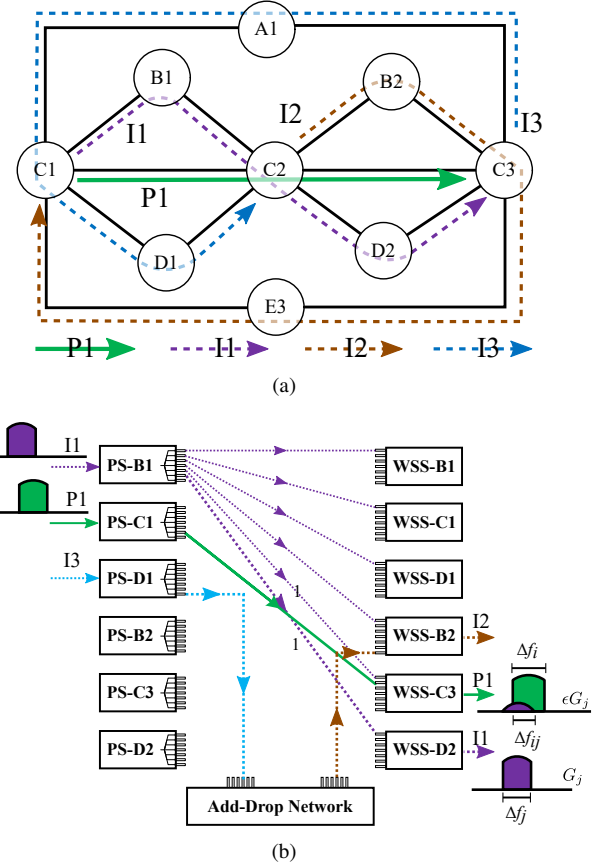


Fig. 2. (a) The 9-node network used to illustrate different forms of AD node crosstalk, (b) Illustration of node crosstalk at node C2 considering a B&S architecture [30]. PS: power splitter (PS).

To analyse the node crosstalk, we assume a broadcast-and-select (B&S) OXC architecture for intermediate node C2 [30], as illustrated in Fig. 2(b). It consists of passive optical splitters (PSs) with $1 \times N$ ports that broadcast signal copies to the common port at local add/drop side and wavelength selective switches (WSSs) facing different output ports and collecting

the signals from add ports. A node crosstalk from signal I1 to P1 arises on WSS-C3 because the broadcast signal I1 is leaked into WSS-C3. We can also observe that the crosstalk signal I3 can leak into P1 on WSS-C3 due to the broadcast function of PS-D1. In addition, we also observe other forms of interference at nodes C1 and C3, which are not shown in Fig. 2(b). When primary signal P1 is added at node C1, it experiences the dropping crosstalk of I2 and the passing-through crosstalk of I3. When the primary signal is dropped at node C3, there is no crosstalk, because P1 is dropped locally. In short, the AD node crosstalk exists if primary signal is added at or passing through the node, and crosstalk signal is passing through or dropped at that node.

Different from the approach of [21] that only supports the node crosstalk by fixed frequency slot, we propose to improve it by adopting the channel bandwidth, which supports arbitrary bandwidth. Thus, assuming the overlapping bandwidth between the primary signal Δf_i and the interfering signal Δf_j is Δf_{ij} , we give the amount of node crosstalk as follows,

$$G_{ijv}^{\text{AD}} = \epsilon \Delta f_{ij} G_j \quad (7)$$

where G_j is the PSD of other interfering signal ($j = 1, 2$ in the example), v is the node C2, and $\Delta f_{ij} = \left| \frac{\Delta f_i + \Delta f_j}{2} - |f_i - f_j| \right|$. In addition, P1 also experiences the crosstalk of I2 at node C1 and the crosstalk of I3 at node C2.

III. TRAFFIC PROVISIONING USING MF AND FEC IN FLEXIBLE OPTICAL NETWORKS

We denote a FON by a graph $G(V, E)$. Each node $v \in V$ represents an OXC. A link $e \in E$ represents two fibers uv and vu ($u, v \in V$) that carry traffic in opposite directions. Each request i is characterized by its source node s_i , destination node d_i , bit-rate r_i (Gbps), PSD G_i ($G_i = G$), and revenue level η_i . The consumed spectrum bandwidth counts $\Delta f_i = r_i / \text{SE}(c_i)$, where $\text{SE}(c_i)$ is the spectral efficiency of transmission mode c_i . Normally, the revenue η_i is determined by the operator's preference or the importance, such as (i) time of day, (ii) duration, (iii) location, (iv) distance, (v) connection speed, and (vi) service type [3]. A random service type parameter is adopted in this paper. Assuming a set of requests in demand D , the total network revenue is the sum of accepted requests' revenue. Available spectrum resource of each fiber is limited to F ($F \in \mathbb{R}^+$).

To serve a request, a lightpath should be established on a continuous and contiguous spectrum interval. We indicate the continuous spectrum interval as $[b_i, e_i]$, where b_i and e_i are the beginning and end of the spectrum interval of request i , respectively. To satisfy the spectrum continuity and contiguity constraints, the spectrum interval $[b_i, e_i]$ must be the same on all traversed links, and can not overlap with other lightpath. Due to limited spectrum resources, not all lightpaths can be provisioned. Therefore, our objective is to maximize the total revenue by optimizing spectrum resource allocation. We use variable B_i to indicate whether request i is served ($B_i = 1$ if it is accepted, 0 otherwise), then the objective function can be expressed by

$$\sum_{i \in D} \eta_i B_i \quad (8)$$

We give an example of revenue difference for different traffic provisioning using transmission mode configurations, *i.e.* single-FEC and multiple-FEC in Fig. 3. Each link has limited spectrum of 100 GHz. The number near each link denotes the length. Three requests R1, R2, and R3 are labeled with source, destination, bit-rate, and revenue. The PSDs for all lightpaths are -11 dBm/GHz.

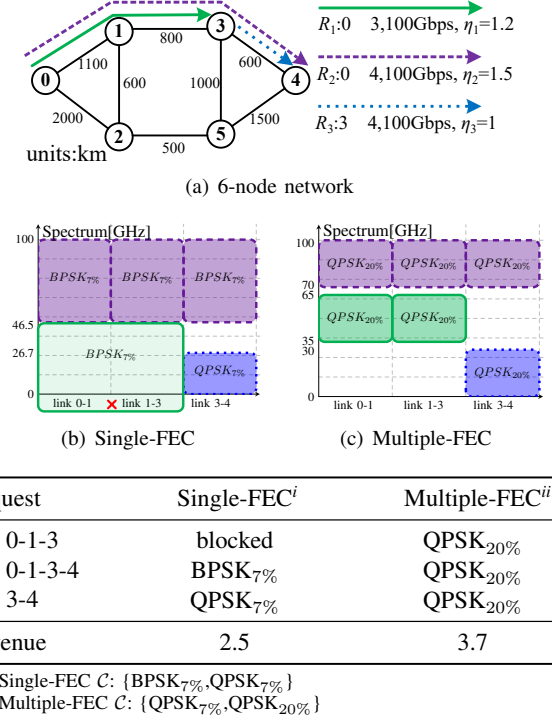


Fig. 3. Traffic provisioning example with single-FEC and multiple-FEC configurations in 6-node network.

In single-FEC configuration, FEC OH is fixed at 7%, hence R2 uses BPSK_{7%} on the channel [46.5, 100], and R3 uses QPSK_{7%} on channel [0, 26.7]. However, the remaining spectrum [0, 46.5] on link 0-1 is not enough to support R1 with BPSK_{7%}. Otherwise, if QPSK_{7%} had been chosen, the QoT of R1 would not have been satisfied because of the fiber nonlinear interference from R2 to R1. Therefore, only two requests can be accepted with single-FEC configuration, leading to a revenue of 2.5.

In multiple-FEC configuration, two FEC OHs can be used. The requests R1, R2, and R3 are served with QPSK_{20%}, as the SNRs with QPSK_{20%} are 6.0 dB, 4.78 dB, and 10.8 dB, respectively, according to Eqs. (2), (4), (5), and (6), which are all over the threshold 4.58 dB. Hence, for multiple-FEC configuration, the revenue is 3.7.

From the example, we see that the revenues can be improved by using multiple-FEC configuration. The traffic provisioning is composed by routing, MF, FEC, and spectrum assignment.

IV. MILP FORMULATION

In this section, we formulate the revenue maximization problem as a MILP, named as RMAX. The parameters and variables of the MILP are summarized in Table II.

TABLE II
PARAMETERS AND VARIABLES IN RMAX

Network Sets and Parameters	
V, E	Node set and link set of the FON G.
$uv \in E$	A link from node u to v .
$s_i, d_i \in V$	Source and destination node of request i .
L_{uv}	Number of spans on link uv .
$F \in \mathbb{R}_{\geq 0}$	Available spectrum resources of an optical fiber.
$N(v)$	Adjacent node set of v in G.
D	Traffic demand matrix.
$i, j \in D$	Any two requests i and j in traffic demand matrix D .
r_i	Required bit-rate (Gbps) of request i .
η_i	Revenue of request i .
$c \in \mathcal{C}$	Transmission mode in candidate transmission mode set \mathcal{C} .
θ	A large constant.
ϵ_1	A factor balancing the importance between revenue and PLIs.
σ_k^1, σ_k^0	Coefficients of piece-wise linear fitting function for fitting the XCI, $k \in \{1, 2, \dots, Q\}$, where Q is the number of segments.
Variables in RMAX	
$B_i \in \{0, 1\}$	Equals 1 if request i is accepted, 0 otherwise.
$q_v^i \in \{0, 1\}$	Equals 1 if request i goes into node v , 0 otherwise.
$p_v^i \in \{0, 1\}$	Equals 1 if request i goes out of node v , 0 otherwise.
$x_{uv}^i \in \{0, 1\}$	Equals 1 if request i uses link uv , 0 otherwise.
$x_{uv,c}^i \in \{0, 1\}$	Equals 1 if request i uses link uv and transmission mode c , 0 otherwise.
$m_c^i \in \{0, 1\}$	Equals 1 if request i uses transmission mode c , 0 otherwise.
$f_i \in [0, F]$	Center frequency of request i .
$f_{ij} \in [0, F]$	Center frequency difference between requests i and j .
$\Delta f_i \in [0, F]$	Bandwidth of request i .
$\Delta f_{ij} \in [0, F]$	Overlapping bandwidth between i and j .
$f_{ij}^X \in [0, F]$	Auxiliary variable of overlapping bandwidth Δf_{ij} .
$w_{ij} \in \{0, 1\}$	Equals 1 if f_i is greater than f_j , 0 otherwise.
$t_{ASE}^i \in \mathbb{R}_{\geq 0}$	PLI of ASE noise of request i , G_i^{ASE}/G_i .
$t_{SCI}^i \in \mathbb{R}_{\geq 0}$	PLI of SCI of request i , G_i^{SCI}/G_i .
$t_{XCI}^i \in \mathbb{R}_{\geq 0}$	Accumulated PLI of XCI of request i from source node s_i to u that is generated by request j .
$t_{ij,v}^{\text{AD}} \in \mathbb{R}_{\geq 0}$	Accumulated PLI of AD node crosstalk of request i from source node s_i to node v that is generated by request j .
h_c^{ij}	Piece-wise linear fitting term for XCI from j to i if j takes transmission mode c .
$t_i^{\text{PLI}} \in \mathbb{R}_{\geq 0}$	Total PLIs of request i .

To provision the lightpaths, both *network flow constraints* and *spectrum assignment constraints* must be taken into account. Besides, *SNR constraints* are also considered to ensure lightpaths' QoT. Thus, the problem is modeled as follows,

$$\max \sum_{i \in D} (\eta_i B_i - \epsilon_1 t_i^{\text{PLI}}) \quad (\text{RMAX})$$

s.t. Constraints (9)-(11).

The main objective of this MILP is to maximize the total revenue and the second objective is to minimize the total PLIs for all requests. The second objective can reduce the PLIs and improve the SNR margin of network, which is regarded as an indirect way that can be used to guarantee the revenue performance [31]. The weighted factor ϵ_1 is used to balance the importance between revenue and PLIs. For the sake of readability, we use $\forall i, \forall v, \forall uv, \forall c$ to denote $\forall i \in D, \forall v \in V, \forall uv \in E, \forall c \in \mathcal{C}$ in the following text.

1) *Network flow constraints*:

$$q_v^i = \sum_{u \in N(v)} x_{uv}^i \quad \forall i, \forall v \quad (9a)$$

$$p_v^i = \sum_{u \in N(v)} x_{vu}^i \quad \forall i, \forall v \quad (9b)$$

$$p_v^i - q_v^i = \begin{cases} B_i, & v = s_i \\ -B_i, & v = d_i \\ 0, & \text{others.} \end{cases} \quad \forall i, \forall v \quad (9c)$$

Constraints (9a) and (9b) determine the incoming and outgoing flow of request i at node v . For any request i , the incoming degree q_v^i counts 1 if request i passes through or drops at node v . Also, for any request i , the outgoing degree p_v^i counts 1 if request i is added at or passes through node v . We will see that, with the help of q_v^i and p_v^i , we can calculate the node crosstalk and other PLIs node-by-node. Constraints (9c) are the flow conservation constraints. If a request i gets accepted ($B_i=1$), there exists a lightpath from the source node s_i to destination node d_i .

2) *Spectrum assignment constraints*:

$$\sum_{c \in \mathcal{C}} m_c^i = B_i \quad \forall i \quad (10a)$$

$$\Delta f_i \geq \sum_{c \in \mathcal{C}} \frac{r_i}{\text{SE}(c)} m_c^i \quad \forall i \quad (10b)$$

$$w_{ij} + w_{ji} = 1 \quad \forall i < j \quad (10c)$$

$$\left. \begin{array}{l} f_i + \Delta f_i/2 \leq F \\ 0 \leq f_i - \Delta f_i/2 \end{array} \right\} \quad \forall i \quad (10d)$$

$$\left. \begin{array}{l} f_{ij} \leq f_i - f_j + 2F(1 - w_{ij}) \\ f_i - f_j \leq f_{ij} \end{array} \right\} \quad \forall i < j \quad (10e)$$

$$\Delta f_{ij} \geq \min(\Delta f_i, \Delta f_j, f_{ij}^X) \quad \forall i < j \quad (10f)$$

$$\Delta f_{ij} \leq F(2 - x_{uv}^i - x_{uv}^j) \quad \forall uv, \forall i < j \quad (10g)$$

$$\left. \begin{array}{l} \Delta f_{ij} = \Delta f_{ji} \\ f_{ij} = f_{ji} \end{array} \right\} \quad \forall i < j \quad (10h)$$

Constraints (10a) select one transmission mode for non-blocked request i (if $B_i = 1$). Constraints (10b) define the bandwidth of request i by its bit-rate and the adopted transmission mode. Constraints (10c) assure that either w_{ij} or w_{ji} should be equal to 1. Constraints (10d) limit the fiber spectrum within $[0, F]$. Constraints (10e) calculate the frequency difference f_{ij} between i and j . Constraints (10f) calculate the overlapping bandwidth Δf_{ij} . As it is not linear, we replace it by the following equations,

$$\begin{aligned} \Delta f_{ij} &\geq \min(\Delta f_i, \Delta f_j, f_{ij}^X) \\ &\left\{ \begin{array}{l} \Delta f_i - Fa_{ij}^1 \leq \Delta f_{ij} \\ \Delta f_j - Fa_{ij}^2 \leq \Delta f_{ij} \\ f_{ij}^X - Fa_{ij}^3 \leq \Delta f_{ij} \\ 0 \leq f_{ij}^X \\ \frac{\Delta f_i + \Delta f_j}{2} - f_{ij} \leq f_{ij}^X \\ f_{ij}^X = f_{ji}^X \\ a_{ij}^1 + a_{ij}^2 + a_{ij}^3 = 2 \\ a_{ij}^1, a_{ij}^2, a_{ij}^3 \in \{0, 1\} \end{array} \right. \quad \forall i < j \end{aligned}$$

Constraints (10g) are spectrum non-overlapping constraints, indicating that when i and j share a common link, the overlapping bandwidth Δf_{ij} on that link must be 0. Constraints (10h) guarantee that both variables Δf_{ij} and f_{ij} are symmetric.

3) *SNR constraints:*

$$t_i^{\text{ASE}} = \sum_{uv} \frac{G_i^{\text{ASE}}}{G_i} L_{uv} x_{uv}^i \quad \forall i \quad (11a)$$

$$t_i^{\text{SCI}} = \sum_{uv} \sum_c \mu G_i^2 L_{uv} \text{arcsinh} \left(\rho \left(\frac{r_i}{\text{SE}(c)} \right)^2 \right) x_{uv,c}^i \quad \forall i \quad (11b)$$

$$x_{uv,c}^i + 1 \geq x_{uv}^i + m_c^i \quad \forall i, \forall c, \forall uv \quad (11c)$$

$$t_{ij,v}^{\text{XCI}} - t_{ij,u}^{\text{XCI}} + \theta(2 - x_{uv}^i - x_{uv,c}^i) \geq \mu G_j^2 h_c^{ij} L_{uv} \quad \forall uv, \forall i \neq j, \forall c \quad (11d)$$

$$t_{ij,v}^{\text{XCI}} - t_{ij,u}^{\text{XCI}} + \theta(1 - x_{uv}^i) \geq 0 \quad \forall uv, \forall i \neq j \quad (11e)$$

$$t_{ij,v}^{\text{AD}} + \theta(3 - p_v^i - q_v^j - m_c^j) \geq \epsilon_{\text{X}}(\Delta f_{ij} G_j) / (r_i / \text{SE}(c) G_i) \quad \forall c, \forall i \neq j, \forall v \quad (11f)$$

$$t_i^{\text{PLI}} \geq t_i^{\text{ASE}} + t_i^{\text{SCI}} + \sum_{j \neq i} t_{ij,d_i}^{\text{XCI}} + \sum_{j \neq i} t_{ij,d_i}^{\text{AD}} \quad \forall i \quad (11g)$$

$$t_i^{\text{PLI}} \leq \sum_{c \in \mathcal{C}} \frac{m_c^i}{\text{SNR}_c^{\text{th}}}, \quad \forall i. \quad (11h)$$

Constraints (11a) calculate PLI of ASE noise on the lightpath. Also, it is applied on the SCI calculation in constraints (11b). Whether request i uses link uv and transmission mode c is assured by the constraints (11c).

Since XCI is caused by two lightpaths, it will increase along their sharing links, and non-decrease along the other links. Constraints (11d) and (11e) implement the XCI calculation, respectively. But the nonlinear expression between XCI and f_i in Eq. (6) makes a nonlinear calculation term h_c^{ij} . To address this issue, we replace the nonlinear term h_c^{ij} by the following linear approximation \hat{h}_c^{ij} ,

$$h_c^{ij} \left(2 \frac{|f_i - f_j|}{\Delta f_j} \right) \geq \ln \left(\frac{2|f_i - f_j|/\Delta f_j + 1}{2|f_i - f_j|/\Delta f_j - 1} \right) \quad (12)$$

$$\Leftarrow \hat{h}_c^{ij}(x) \geq \max(o_1^1 x + o_1^0, \dots, o_k^1 x + o_k^0, \dots, o_Q^1 x + o_Q^0)$$

$$\Leftarrow \hat{h}_c^{ij} \geq o_k^1 (2\text{SE}(c) f_{ij} / r_j) + o_k^0 \quad \forall i \neq j, \forall c, 1 \leq k \leq Q$$

where o_k^1 and o_k^0 are the coefficients solved by piece-wise linear fitting. We use the least-square algorithm in [32] to fit the convex function $\ln \left(\frac{x+1}{x-1} \right)$ in the domain $x \in [x_1, x_2]$, where we set $x_1=1.001$, $x_2=200$, and $Q=20$. The fitting error $(\hat{h}_c^{ij} - h_c^{ij})/h_c^{ij}$ can be minimized by increasing the number of segments Q . As shown in Fig. 4, the maximum fitting error is less than 5%.

Constraints (11f) calculate the node crosstalk along the lightpath, which is implemented by emphasizing the incoming degree q_v^j of crosstalk signal j and the outgoing degree p_v^i of primary signal i . Constraints (11g) calculate the total PLIs of all traversed links and nodes. Constraints (11h) represent the QoT formulation. The MILP is NP hard and time-consuming [22]. Considering the scalability limitations of MILP, we also

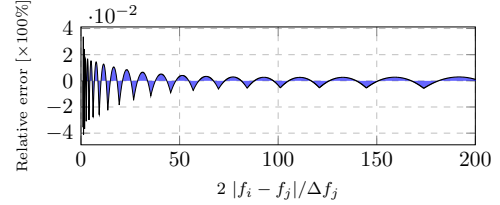


Fig. 4. Illustration for the piece-wise linear fitting performance, $(\hat{h}_c^{ij} - h_c^{ij})/h_c^{ij}$ versus $2|f_i - f_j|/\Delta f_j$, $Q=20$.

design a heuristic algorithm to solve the revenue maximization problem with lower complexity.

V. HEURISTIC ALGORITHMS

In this section, we design a decomposition algorithm (DEC-ALG) to solve (a) the problem of routing, MF, and FEC assignment, and (b) the problem of spectrum assignment, separately. In addition, we also present a heuristic as benchmark, which is adapted from existing literature.

A. DEC-ALG

DEC-ALG algorithm consists of two phases: (a) Routing and transmission mode assignment (RTMA); (b) Spectrum assignment (SA). The related parameters and variables are explained in Table III.

TABLE III
PARAMETERS & VARIABLES IN ALGORITHM DEC-ALG

Network sets & Parameters	
$\phi \in [0, 1]$	A ratio on SNR threshold considering ASE+SCI. $1 - \phi$ represents the part considering XCI+AD.
P_i	Route and transmission mode pairs set (ξ, c) of request i .
P_{ie}	Route and transmission mode pairs set (ξ, c) of request i that traverses link e .
$V_{i\xi}$	Node set on the ξ -th route of request i .
ϵ_2	Factors adjusting the weight of rest SNR margin.
b_i, e_i	Spectrum beginning and end of request i .
$\phi_{i\xi c} \in \mathbb{R}$	SNR margin of request ξ using transmission mode c and ξ -th route after RTMA.
Δf_{ic}	Bandwidth of request i using transmission mode c .
N_{RTMA}	Number of RTMA_{opt} solutions.
N_{round}	Number of attempts in the spectrum assignment.
Variables	
$B_i \in \{0, 1\}$	Equals 1 if request i is accepted, 0 otherwise.
$g_{i\xi c} \in \{0, 1\}$	Equals 1 if request i uses the ξ -th route and transmission mode c , 0 otherwise.
ϕ_{avg}	Average SNR margin of all requests.

1) *Pre-calculation process:* We pre-calculate route and transmission mode pairs for each request. Candidate routes are obtained by the K shortest path algorithm [33], while transmission modes are from \mathcal{C} .

For any request i , the tuple (ξ_i, c_i) denotes a route and transmission mode pair. The ASE and SCI are the known impairments for a given (ξ_i, c_i) , which are obtained by Eqs. (4) and (5). However, the node crosstalk and XCI can not be determined because they are related with the exact spectrum channel of all lightpaths. Thus, some route and transmission mode pairs may experience strong PLIs, thus the QoT cannot

be satisfied in the subsequent process. Therefore, we choose the route and transmission mode pair (ξ, c) based on the residual SNR margin $\phi_{i\xi c}$ as follows,

$$\phi_{i\xi c} = \frac{\phi}{\text{SNR}_c^{\text{th}}} - t_i^{\text{ASE}} - t_i^{\text{SCI}} - \epsilon_X \sum_{v \in V_{i\xi}} \frac{N(v) + 1}{2} \quad (13)$$

where ϕ is an estimated ratio considering the ASE and SCI.

2) **RTMA**: In RTMA, each request can choose one route and transmission mode pair (ξ, c) . For all requests, one assignment of the route and transmission mode pair, named as RTMA_{opt} , is solved by the following RTMA model,

$$\max \sum_{i \in D} \eta_i B_i + \epsilon_2 \phi_{\text{avg}} \quad (\text{RTMA})$$

$$\text{s.t.} \quad \sum_{(\xi, c) \in P_i} g_{i\xi c} = B_i \quad \forall i \quad (14a)$$

$$\sum_{i \in D} \sum_{(\xi, c) \in P_{ie}} \Delta f_{ie} g_{i\xi c} \leq F \quad \forall e \quad (14b)$$

$$0 \leq \sum_{(\xi, c) \in P_i} g_{i\xi c} \phi_{i\xi c}, \quad \forall i \quad (14c)$$

$$\phi_{\text{avg}} = \frac{1}{|D|} \sum_{i \in D} \sum_{(\xi, c) \in P_i} g_{i\xi c} \phi_{i\xi c} \quad (14d)$$

The main objective of RTMA is to maximize the accepted revenue and the second one is to maximize average SNR margin. The multi-objective function can be adjusted by weighting factor ϵ_2 . Constraints (14a) make sure that a route and transmission mode pair (ξ, c) is chosen for request i if $B_i=1$. Constraints (14b) restrict the spectrum usage of each link. Bandwidth requirement of i with the transmission mode c has been pre-calculated and denoted by Δf_{ie} . Constraints (14c) make sure that the minimum SNR margin is non-negative. Constraint (14d) defines the average SNR margin of all requests.

In RTMA, only one RTMA_{opt} solution is obtained. However, this solution may not bring the maximum revenue after spectrum assignment. To this end, we intend to generate N_{RTMA} solutions. The n -th solution is generated by adding constraints (15) to RTMA, which is used for excluding the previous RTMA_{opt} . In constraints (15), both B_i^{n-1} and $g_{i\xi c}^{n-1}$ are the results from $(n-1)$ -th solution.

$$\begin{aligned} & \sum_{\substack{i \in D \\ B_i^{n-1}=1 \\ g_{i\xi c}^{n-1}=1}} \sum_{(\xi, c) \in P_i} g_{i\xi c} + \frac{1}{K * |\mathcal{C}|} \sum_{\substack{i \in D \\ B_i^{n-1}=0 \\ g_{i\xi c}^{n-1}=0}} \sum_{(\xi, c) \in P_i} (1 - g_{i\xi c}) \\ & \leq |D| - \frac{1}{K * |\mathcal{C}|}, n \in \{1, 2, 3, \dots, N_{\text{RTMA}}\} \end{aligned} \quad (15)$$

Explanation of excluding constraints (15) : In the n -th loop, we suppose that $\forall i, (\xi, c)$, the variable $g_{i\xi c} = g_{i\xi c}^{n-1}$, then the value of the left side in constraints (15) becomes $|D|$, which is larger than the right. Therefore, we can say that constraints (15) hold if $\exists i, (\xi, c), g_{i\xi c} \neq g_{i\xi c}^{n-1}$. Let us focus on the request i that satisfies $g_{i\xi c} \neq g_{i\xi c}^{n-1}$. Since constraints

(14a) require $\sum_{(\xi, c)} g_{i\xi c}^{n-1} = B_i^{n-1} \leq 1$, we discuss the case $B_i^{n-1} = 1$ and $B_i^{n-1} = 0$, respectively.

- If $B_i^{n-1} = \sum_{(\xi, c)} g_{i\xi c}^{n-1} = 1$ holds,

$$\left. \begin{array}{l} B_i^{n-1} = \sum_{(\xi, c)} g_{i\xi c}^{n-1} = 1 \\ \exists (\xi, c), g_{i\xi c} \neq g_{i\xi c}^{n-1} \\ \sum_{(\xi, c)} g_{i\xi c} \leq 1 \end{array} \right\} \Rightarrow \sum_{\substack{(\xi, c) \in P_i \\ g_{i\xi c}^{n-1}=1}} g_{i\xi c} = 0 \quad (16)$$

- Otherwise $B_i^{n-1} = \sum_{(\xi, c)} g_{i\xi c}^{n-1} = 0$ holds, then we can get the result $\frac{1}{K * |\mathcal{C}|} \sum_{(\xi, c) \in P_i} (1 - g_{i\xi c}) = \frac{K * |\mathcal{C}| - 1}{K * |\mathcal{C}|} < 1$ with the following proof,

$$\left. \begin{array}{l} B_i^{n-1} = \sum_{(\xi, c)} g_{i\xi c}^{n-1} = 0 \\ \exists (\xi, c), g_{i\xi c} \neq g_{i\xi c}^{n-1} \\ \sum_{(\xi, c)} g_{i\xi c} \leq 1 \end{array} \right\} \Rightarrow \left\{ \begin{array}{l} \sum_{(\xi, c) \in P_i} g_{i\xi c} = 1 \\ g_{i\xi c}^{n-1}=0 \\ \sum_{(\xi, c) \in P_i} (1 - g_{i\xi c}) = K * |\mathcal{C}| - 1 \\ g_{i\xi c}^{n-1}=0 \end{array} \right. \quad (17)$$

In addition, for the request i that satisfies $\forall (\xi, c), g_{i\xi c} = g_{i\xi c}^{n-1}$, the first item of left sides still equals 1. The number is denoted by n_1 , $n_1 \leq |D| - 1$. Thus, we can get $0 \cdot n_{(16)} + 1 \cdot n_1 + (1 - 1/K * |\mathcal{C}|) \cdot n_{(17)} \leq |D| - 1/K * |\mathcal{C}|$, where $n_{(16)}$ and $n_{(17)}$ are the number of requests satisfying (16) and (17), respectively, and $n_{(16)} + n_1 + n_{(17)} = |D|$. Therefore, the left side of constraints (15) must be no bigger than $|D| - \frac{1}{K * |\mathcal{C}|}$.

The pseudo code in Algorithm 1 illustrates the procedure of generating N_{RTMA} solutions by RTMA. In line 1, the model is initialized with the constraints (14) and the input parameters $G(V, E)$, D , N_{RTMA} , and \mathcal{C} . In line 2, RTMA_{opt} solution with $g_{i\xi c} = 0$ is initialized. Then, from lines 3 to 5, the RTMA model is repeated to get N_{RTMA} solutions.

Algorithm 1: RTMA: generating N_{RTMA} solutions

Input : $G(V, E)$, D , N_{RTMA} , \mathcal{C}

Output: $g^{N_{\text{RTMA}}}$

- 1 Create the RTMA model with the constraints in (14) and the input parameters $G(V, E)$, D , N , and \mathcal{C} ;
- 2 $g_{i\xi c}^0 \leftarrow 0, \forall i, (\xi, c) // g_{i\xi c}^0 \in g^0$
- 3 **for** $n \in \{1, 2, \dots, N_{\text{RTMA}}\}$ **do**
- 4 | Update the RTMA model with excluding constraints (15) and previous solution g^{n-1} ;
- 5 | Get the RTMA_{opt} solution g^n by solving RTMA model;

3) **SA**: Once the RTMA problem is solved, from the solution RTMA_{opt} , we can obtain the pair index of route and transmission mode used for each request i , i.e., $(\bar{\xi}_i, \bar{c}_i) = \{(\xi, c) | g_{i\xi c} = 1, i \in D\}$.

When assigning the spectrum interval on the determined route for each request, SA needs to take into account both spectrum continuity and spectrum contiguity constraints. To reduce the impact of XCI, we also set a guard band $\Delta=12.5$

GHz. If the request is accepted, a specific lightpath with its spectrum interval will be allocated. Otherwise, it will move the spectrum interval when necessary until it is out of the fiber spectrum. A new incoming request can be blocked if it affects the QoT of other requests. To ensure the blocked requests can be accepted again, we repeat the assignment process N_{round} times. For the request in each round, the SNR threshold is designed to decrease gradually, and equals to the SNR threshold of transmission mode c in the final round.

The SA procedure is illustrated in Algorithm 2. In line 1, we sort the requests in D by function **ARRANGE**, which will be explained later. Then, in lines 5 and 6, the required spectrum bandwidth and route can be both found from the RTMA result RTMA_{opt} . In line 7, we merge the available spectrum of the ξ -th route and assign it to $\text{MERGED}_{\text{space}}$, where both spectrum continuity and spectrum contiguity constraint are satisfied. Then, from lines 8 to 16, the algorithm SA tries to search a spectrum interval $[b_i, b_i + \Delta f_i]$ from $\text{MERGED}_{\text{space}}$ that satisfies the QoT.

In the **ARRANGE** function of Algorithm 2, we sort the requests in D by four different assignment policies, *random order* Δf_i (SA), *descending order of bandwidth* Δf_i (SA-B), *revenue* η_i (SA-R), and *revenue to bandwidth ratio* $\eta_i/\Delta f_i$ (SA-RA), respectively. The performances of these four arrangement policies are compared in simulations.

Algorithm 2: SA : Spectrum Assignment

```

Input :  $g$ 
Output:  $alloc$ 
1  $D_{\text{arr}} \leftarrow \text{ARRANGE}(D);$ 
2  $alloc \leftarrow 0$  //  $alloc_i \in alloc$ ;
3 for  $n_{\text{round}} \in [0, 1, \dots, N_{\text{ROUND}}]$  do
4   for  $i \in D_{\text{arr}}$  &  $alloc_i == 0$  do
5      $(\bar{\xi}_i, \bar{c}_i) \leftarrow \{(\xi, c) | g_{i\xi c} = 1\}$  //  $g_{i\xi c} \in g$ ;
6      $\Delta f_i \leftarrow r_i / \text{SE}(\bar{c}_i)$  ;
7      $\text{MERGED}_{\text{space}} \leftarrow$  available spectrum space on
       $\bar{\xi}_i$ -th route;
8     for the spectrum beginning  $b_i: 0 \rightarrow F$ , with step
       $\Delta = 12.5 \text{ GHz}$  &  $alloc_i == 0$  do
9       if  $[b_i, b_i + \Delta f_i] \in \text{MERGED}_{\text{space}}$  then
10         try :
11           Assign  $[b_i, b_i + \Delta f_i]$  on  $\bar{\xi}_i$ -th route;
12           Check QoT of assigned requests by
             Eq. (3);
13           Check QoT of current request  $i$  by
             Eq. (3);
14            $alloc_i \leftarrow 1$ ;
15         catch Check failed:
16            $alloc_i \leftarrow 0$ ;

```

4) **DEC-ALG**: It is worth mentioning that the size of RTMA_{opt} solution space can reach $(K \cdot |\mathcal{C}| + 1)^{|D|}$. With small N_{RTMA} , i.e. $N_{\text{RTMA}} \ll (K \cdot |\mathcal{C}| + 1)^{|D|}$, the potential RTMA_{opt} solution that provides the maximum revenue may not be included. In addition, the solution space of RTMA is

determined by the number of routes K , the size of candidate transmission mode \mathcal{C} and demand D . It may happen that we get the identical result even with different configurations \mathcal{C}' or different demand matrix D' .

To solve the problem caused by different transmission mode configurations \mathcal{C} , we use a perturbation strategy to extend RTMA_{opt} solutions by its subset, \mathcal{C}_l^{sub} , $1 \leq l \leq |\mathcal{C}|$. Each subset takes l elements from \mathcal{C} . For the l -th subset \mathcal{C}_l^{sub} , the l -th transmission mode of \mathcal{C} is added compared to the previous $l - 1$ subsets. Constraints (18) are used to generate RTMA_{opt} for the subset \mathcal{C}_l^{sub} that forces the use of transmission mode c^l but excludes the use of the other transmission modes c^r .

$$\sum_{i \in D, 1 \leq \xi \leq K} g_{i\xi c^l} \geq 1 \quad (18a)$$

$$\sum_{i \in D, 1 \leq \xi \leq K} g_{i\xi c^r} = 0, \forall c^r \in \mathcal{C} \setminus \mathcal{C}_l^{sub} \quad (18b)$$

We give the pseudo code of DEC-ALG as illustrated in Algorithm 3. In line 2, we initialize the candidate transmission sets \mathcal{C}_l^{sub} . From lines 3 to 7, we conduct the algorithm RTMA and SA to obtain the optimal result. Finally, the maximum revenue MAXOBJ is saved.

Algorithm 3: DEC-ALG

```

Input :  $G(V, E), D, N_{\text{RTMA}}, \mathcal{C}$ 
Output: MAXOBJ
1  $\text{MAXOBJ} \leftarrow 0$ ;
2 for  $c^l \in \mathcal{C}$  do
3   Initialize the current transmission mode set  $\mathcal{C}_l^{sub}$ ;
4   Use RTMA model to generate  $\text{RTMA}_{\text{opt}}(G, D,$ 
       $N_{\text{RTMA}}, \mathcal{C})$  solutions, with constraints (18)
      emphasising the lock transmission mode  $c^l$ ;
5   for  $n \in \{0, 1, \dots, N_{\text{RTMA}}\}$  do
6      $alloc \leftarrow \text{SA}(g^n)$  //  $alloc_i \in alloc$ 
7      $\text{Obj} \leftarrow \sum_i alloc_i * \eta_i$  ;
8      $\text{MAXOBJ} \leftarrow \max(\text{Obj}, \text{MAXOBJ})$ ;

```

B. Benchmark algorithm

To efficiently utilize the spectrum resource of fiber, a large number of algorithms on traffic provisioning have been proposed [8, 34]. To make a fair comparison, we take the algorithm in [8] that also adopts the continuous spectrum allocation. The benchmark algorithm, called as REF-A in this paper, is implemented by using the same objective function of RTMA in Eq. (14) and restricting the fiber spectrum resources. It should be also noted that, the spectrum assignment of REF-A is implemented by passing the solution of RTMA to RMAX.

VI. ILLUSTRATIVE NUMERICAL RESULTS

In this section, we present the numerical experiment results. First, we compare the efficiency of our proposed heuristic and the MILP model. Then, we investigate revenues in scenarios with different PSDs and different transmission modes. Finally, we consider the experiments for severe resource crunch, which is simulated by increasing bit-rate and number of requests.

The MILP, heuristic algorithm DEC-ALG, and REF-A run on an Intel Core PC with 4.0 GHz CPU and 16 GB RAM. Specifically, we solved the MILP model by CPLEX 12.6 and implemented the two heuristic algorithms using an ad-hoc code developed in C++. Maximum computing time for the MILP was fixed to one hour. All illustration results have been averaged over 10 independent simulation runs to guarantee statistical accuracy.

The 6-node network in Fig. 3, NSFNET (14 nodes, 44 links) [35], and US Backbone network (28 nodes, 90 links) [35] are used as case study topologies (note that, since the path length of NSF network and US Backbone network cannot support high-order MF, we divide the length of link by 6 in the simulations). The spectrum resource of each fiber F is assumed with 1,000 GHz to increase the simulation speed for large networks. The fiber parameters α , β_2 , and γ are from Table I. The algorithm parameter $\epsilon_1=0.01$ and $\epsilon_2=0.001$ are adjusted to be small to emphasize the revenue rather than the other parameters for simulation. The parameters $N_{RTMA}=40$, $N_{round}=2$, and $K=4$ are adjusted to guarantee stable good simulation results in a reasonable time. The bit-rates r_i are randomly chosen from the set $\{250, 500, \dots, 250+n*250, \dots, 250+2n*250\}$ Gbps. For the lowest bit-rate, the channel can be guaranteed with bandwidth over than 28 GHz with PM-16QAM [8], which is acceptable for the GN model in [28]. The large bit-rate request is assumed by super-channel with large baud rates. The initial launch power PSD for all lightpaths is simplified with -16 dBm/GHz by using the LOGON strategy [36] for one span with the heaviest spectral loads. The definition of revenue and other used notations for simulation are given as follows,

- 1) *Revenue*: $\eta_i = u_i$, where u_i is the service type parameter. In this paper, we consider the service type parameter u_i follows the Zipf distribution $Zipf(1,5)$ [37]. The revenue of a network is sum of all accepted lightpaths' revenue.
- 2) *Adaptive MFs* : $\mathcal{C} = (\hat{\mathcal{M}}_m, \mathcal{F}_f)$. Notation \mathcal{F}_f represents one f -th level FEC, and $\hat{\mathcal{M}}_m$ represents all the MFs not beyond the m -th order.
- 3) *Multiple FECs*: $\mathcal{C} = (\mathcal{M}_m, \hat{\mathcal{F}}_f)$. Notation \mathcal{M}_m represents the m -th order MF, and $\hat{\mathcal{F}}_f$ represents the FEC OHs not beyond the f -th one.

A. Validation using MILP

We validate the MILP on the 6-node network. The bit-rate per request is fixed at 1,000 Gbps. Figure 5 illustrates the revenue and computational time of three algorithms as the number of request increases.

In Fig. 5, we can observe that the computational time of MILP reaches the preset maximum computing time one hour, when the number of requests increases to 33. It means that MILP is intractable even in the case with either small networks or small number of requests. But the heuristic algorithm REF-A and DEC-ALG can solve it in a few minutes and a few seconds, respectively. Besides, we observe that both DEC-ALG and REF-A are able to obtain an approximate optimal value of MILP. Therefore, the proposed algorithm DEC-ALG is not only time-efficient but also near-optimal.

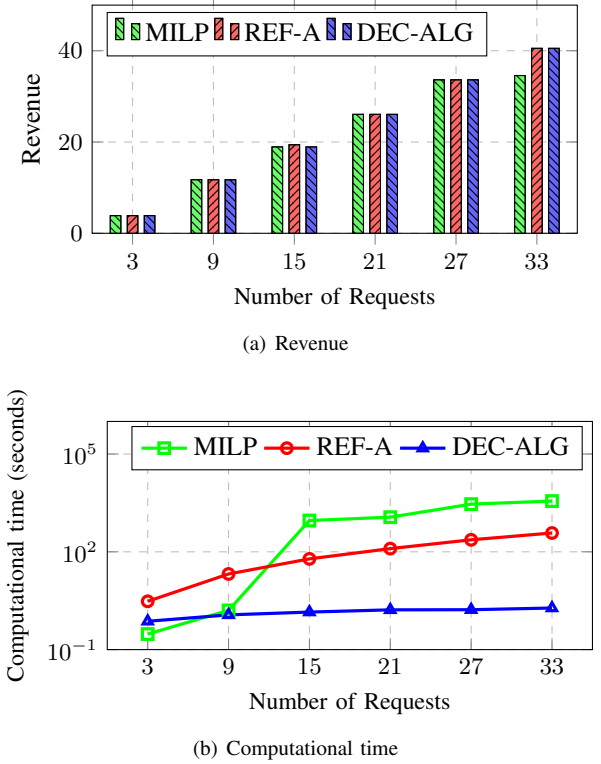


Fig. 5. Comparison of revenue and computational time in 6-node network.

In the SA of DEC-ALG algorithm, we have mentioned four different sorting policies in the ARRANGE function. In order to find the best sorting policy, we compared their results in Fig. 6. The simulation is carried out in NSF network. As we see in Fig. 6, the revenue with different sorting policies increases with the number of requests. It can be also seen that SA-RA, which sorts the requests by the descending order of revenue/bandwidth ratio, gets the largest revenue. Therefore, we confirm to use SA-RA for heuristic algorithm DEC-ALG.

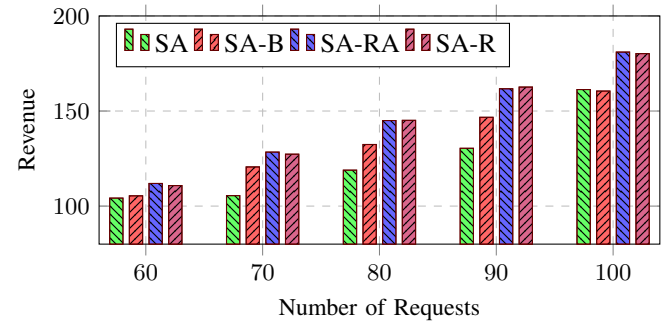


Fig. 6. Revenue comparison with four different sorting policies of ARRANGE function.

B. Impacts of PSD, MF and FEC

As we have seen in the example of Fig. 3, revenues can be influenced by SNR requirements of different transmission mode configurations. In Eqs. (3), (4) and (5), when PSD G_i increases, the noise to signal ratio of ASE, t_i^{ASE} will decrease

inversely, while the t_i^{SCI} and t_i^{XCI} will increase quadratically. The PSD of ASE noise, SCI, and XCI, as well as the SNR for a 250 Gbps request with PM-QPSK7% in the middle of a fully occupied fiber span are illustrated in Fig. 7. According to the SNR and PSD, we briefly distinguish three different scenarios, namely scenario 1: *low SNR with low PSD*, scenario 2: *high SNR with median PSD*, and scenario 3: *low SNR with high PSD*. By adjusting PSDs, we can investigate the revenue impact of MF and FEC in different SNR scenarios.

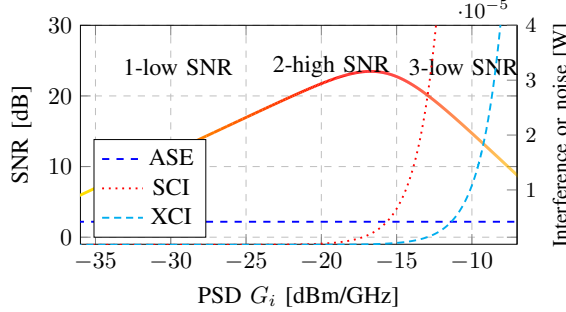


Fig. 7. SNR vs. PSD G_i .

First, we fix FEC OH at 7% and compare different MFs as PSD varies. The simulation results of NSF network using 100 requests and 1,000 Gbps per request are illustrated in Fig. 8(a). It is observed in Fig. 8(a) that the revenue of different MFs increases as PSD changes from scenario 1 to 2, but then decreases from scenario 2 to 3. Both adaptive MF $\hat{\mathcal{M}}_3$ and $\hat{\mathcal{M}}_4$ that contain MFs {BPSK,QPSK,8QAM} get the largest revenue in scenario 2, with 118% improvement compared to $\hat{\mathcal{M}}_1$. It can be explained by the SNR threshold and spectral efficiency of different MFs. Only in the scenario with high SNR, high-order MFs can be adopted, which reduces the spectrum usage and spares more spectrum resources for other requests. However, in the scenario with low SNR, the adaptive method with four MFs has no difference with either one MF or two MFs, because the high-order MF cannot be adopted.

Then, we fix MF at QPSK and compare multiple FECs. The results are illustrated in Fig. 8(b), where we can see that, also in this case, as PSD changes from scenario 1 to 2, the revenue of different FECs increases, while from scenario 2 to 3, the revenue decreases. Different from the adaptive MF, having multiple FEC choices has a tiny impact on revenue difference on scenario 2, while a bigger difference is only observed for both scenarios 1 and 3, which is a different result with respect to adaptive MF. In low SNR scenario, most lightpaths with small FEC OHs are blocked, while the redundant FEC with large FEC OHs can lower the SNR requirement and provide more SNR margins to overcome the PLIs. But in high SNR scenario, many requests have adopted the transmission mode f_1 with the highest spectral efficiency. Therefore, no revenue improvement can be observed in this scenario.

Figures 8(a) and 8(b) indicate that adaptive MF brings more revenue in high SNR with median PSD, while multiple FECs configuration brings more revenue in low SNR scenarios. As we introduce more MFs and FEC, the high-order MF will mitigate the resource crunch and the low-spectral efficiency

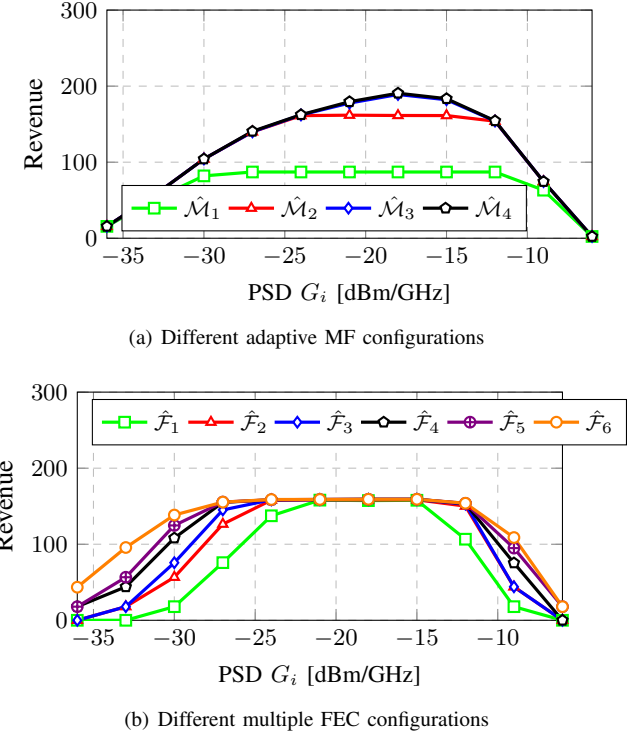


Fig. 8. Impact of PSD.

FEC with large OH can mitigate the PLIs.

Given suitable PSD scenario of multiple FECs and adaptive MF, we further investigate the impact of joint MF and FEC schemes in NSF and US Backbone network. The revenues of 100 requests with average bit-rate 1,000 Gbps are illustrated in Fig. 9. In high SNR scenario with median PSD ($G_i = -18$ dBm/GHz), we find that the adaptive MFs enable to improve the revenue, while the configuration of multiple FECs has weak impact on the revenue. In low SNR scenario with high PSD ($G_i = -9$ dBm/GHz), both adaptive MFs and multiple FECs enable to improve the revenue, which means that the combination of MF and FEC is preferred in high PSD scenario rather than median PSD scenario. We also find that the revenue of adaptive MF configuration $\hat{\mathcal{M}}_3$ and multiple FEC configuration $\hat{\mathcal{F}}_5$ can reach the almost maximum value for both high and low SNR scenarios. It means that the usage of MF with PM-16QAM and FEC OH with 50% can be saved.

C. Different traffic loads

Let us now study the impact of different numbers of requests. The simulations assume all requests with identical 1,000 Gbps [8]. The PSD is either -18 dBm/GHz or -9 dBm/GHz, such that we operate in scenarios that benefit of adaptive MFs and multiple FECs, respectively. The results of different adaptive MFs and different FECs are shown in Fig. 10(a) and 10(b). In Fig. 10(a), the four adaptive MFs obtain the same result with 20 requests, but, as the number of requests increases, the gain achieved by using four different adaptive MFs also increases. The maximum improvement of adaptive MFs (186% higher compared to $\hat{\mathcal{M}}_1$) is obtained with 200 requests. In Fig. 10(b), multiple FECs' revenue also

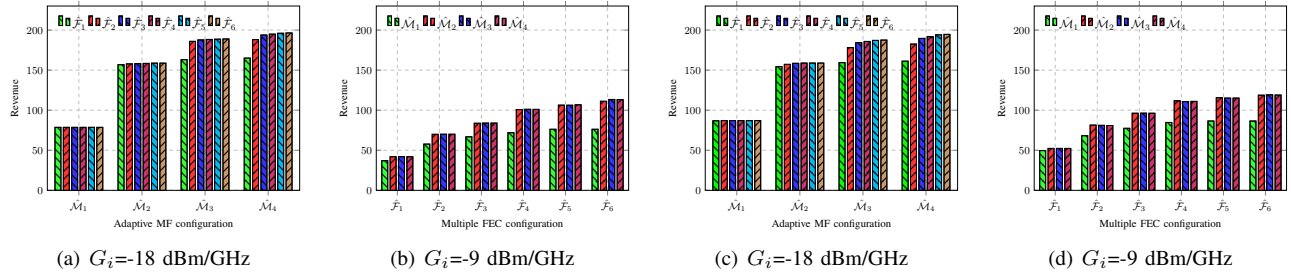


Fig. 9. Revenue impact of joint MF and FEC. (a) and (b) are in NSF network; (c) and (d) are in US Backbone network.

increases with the number of requests. Configuration $\hat{\mathcal{F}}_6$ gets the largest revenue, which is 3.6 times higher than $\hat{\mathcal{F}}_1$.

We report the simulation results with different average bit-rates in Fig. 11. For a given average bit rate of $250+n*250$, each request can randomly chose the bit-rate from the set $\{250, \dots, 250+2n*250\}$. 160 requests are assumed in the simulation. The results of different MFs and FECs are shown in Figs. 11(a) and 11(b). We observe that the revenue decreases with the average bit-rate. The larger the bit-rate, the more spectral resources' consumption of fiber, which leads to blocked requests. For the case with more transmission modes, such as $\hat{\mathcal{M}}_4$ or $\hat{\mathcal{F}}_6$, it can also gain more revenue compared to the other configuration with fewer transmission modes, $\hat{\mathcal{M}}_1$ or $\hat{\mathcal{F}}_1$. When the average bit-rate increases to 1,500 Gbps, the revenue improvement ratio of $\hat{\mathcal{M}}_4$ and $\hat{\mathcal{F}}_6$ reaches about 98% and 362% compared to $\hat{\mathcal{M}}_1$ and $\hat{\mathcal{F}}_1$, respectively.

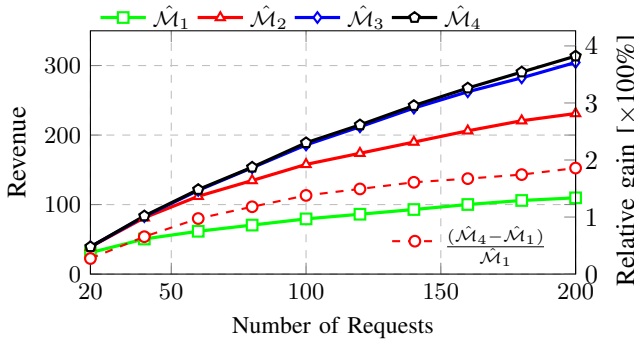


Fig. 10. Revenue impact with the number of requests in NSF network. Bit rate per request is 1,000 Gbps.

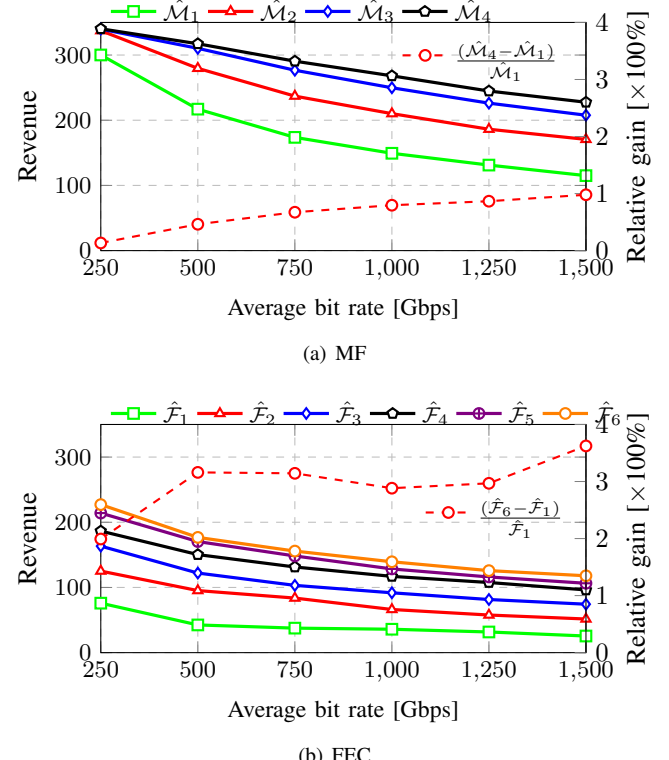


Fig. 11. Revenue impact with different traffic rates in NSF network. The simulations use 160 requests.

VII. CONCLUSION

In this paper, we studied the problem of using adaptive MFs and multiple FECs to improve the traffic provisioning in FONs. The objective is to maximize the total network revenue. To this end, we develop a MILP model and a fast two-phase heuristic algorithm, which is shown to be near-optimal for revenue maximization. Although the revenue loss is inevitable under different resource crunch scenarios, it can be improved by properly choosing the transmission mode configurations and physical parameters. Through simulations, we demonstrate that using adaptive MF enables to increase the revenue more than 100% in the scenario of high SNR while using adaptive FEC is profitable for scenarios with low SNR. While guaranteeing the revenue performance, the usage of adaptive MF configuration with PM-16QAM and multiple FEC configuration with OH 50% can be saved. We also carry out experiments to demonstrate the case of severe resource

crunch, which is simulated by increasing bit-rate and number of requests. It shows that for the case of high traffic load (large number of requests or big average bit-rate), adaptive MF takes more advantage than single MF with PM-BPSK, because it can offer more spectrum-efficient transmission modes.

ACKNOWLEDGMENT

The work is jointly supported by Eiffel Scholarship (No. 895145D), open project (2020GZKF017) of Shanghai Jiao Tong University. China Scholarship Council (No. 201806230093), National Nature Science Fund of China (No.61775137, No.62071295, No.61431009, and No.61433009), National “863” Hi-tech Project of China (No.2013AA013602 and No.2012AA011301), and NSF (Grant No. 1716945).

REFERENCES

- [1] C. Chen, F. Zhou, and S. Xiao, “Maximizing revenue with adaptive modulation and multiple FEC in flexible optical networks,” in *Proc. Conf. on High Perform. Comput. and Commun. (HPCC)*, Zhangjiajie, China, Aug. 2019, pp. 2476–2481.
- [2] “Cisco visual networking index: Forecast and trends, 2017–2022,” Cisco, Tech. Rep., Nov. 2018.
- [3] R. B. Lourenço, M. Tornatore, C. U. Martel, and B. Mukherjee, “Running the network harder: connection provisioning under resource crunch,” *IEEE Trans. Netw. Service Manag.*, Oct. 2018.
- [4] Z. Zhong, N. Hua, M. Tornatore, J. Li, Y. Li, X. Zheng, and B. Mukherjee, “Provisioning short-term traffic fluctuations in elastic optical networks,” *IEEE/ACM Trans. Netw.*, vol. 27, no. 4, pp. 1460–1473, Aug. 2019.
- [5] D. D. Le, F. Zhou, and M. Molnár, “Minimizing blocking probability for the multicast routing and wavelength assignment problem in WDM networks: Exact solutions and heuristic algorithms,” *IEEE/OSA J. Opt. Commun. Netw.*, vol. 7, no. 1, pp. 36–48, Jan. 2015.
- [6] M. Klinkowski and K. Walkowiak, “Routing and spectrum assignment in spectrum sliced elastic optical path network,” *IEEE Commun. Lett.*, vol. 15, no. 8, pp. 884–886, Aug. 2011.
- [7] C. Rottondi, M. Tornatore, A. Pattavina, and G. Gavioli, “Routing, modulation level, and spectrum assignment in optical metro ring networks using elastic transceivers,” *IEEE/OSA J. Opt. Commun. Netw.*, vol. 5, no. 4, pp. 305–315, Apr. 2013.
- [8] L. Yan, E. Agrell, M. N. Dharmawewa, and H. Wymeersch, “Joint assignment of power, routing, and spectrum in static flexible-grid networks,” *IEEE/OSA J. Lightw. Technol.*, vol. 35, no. 10, pp. 1766–1774, May 2017.
- [9] K. Manousakis, K. Christodoulopoulos, E. Kamitsas, I. Tomkos, and E. A. Varvarigos, “Offline impairment-aware routing and wavelength assignment algorithms in translucent WDM optical networks,” *IEEE/OSA J. Lightw. Technol.*, vol. 27, no. 12, pp. 1866–1877, Jun. 2009.
- [10] N. Sambo, G. Meloni, F. Cugini, F. Fresi, A. D’Errico, L. Poti, P. Iovanna, and P. Castoldi, “Routing, code, and spectrum assignment, subcarrier spacing, and filter configuration in elastic optical networks,” *IEEE/OSA J. Opt. Commun. Netw.*, vol. 7, no. 11, pp. B93–B100, Nov. 2015.
- [11] A. Alvarado, D. J. Ives, S. J. Savory, and P. Bayvel, “On the impact of optimal modulation and FEC overhead on future optical networks,” *IEEE/OSA J. Lightw. Technol.*, vol. 34, no. 9, pp. 2339–2352, Jan. 2016.
- [12] G. Bosco, “Advanced modulation techniques for flexible optical transceivers: The rate/reach trade-off,” *IEEE/OSA J. Lightw. Technol.*, vol. 37, no. 1, pp. 36–49, Jan. 2019.
- [13] H. Khodakarami, B. S. G. Pillai, B. Sedighi, and W. Shieh, “Flexible optical networks: an energy efficiency perspective,” *IEEE/OSA J. Lightw. Technol.*, vol. 32, no. 21, pp. 3356–3367, Jun. 2014.
- [14] L. Velasco, M. Ruiz, J. Perelló, S. Spadaro, and J. Comellas, “Service and resource differentiation in shared-path protection environments to maximize network operator’s revenues,” *IEEE/OSA J. Opt. Commun. Netw.*, vol. 3, no. 2, pp. 117–126, Feb. 2011.
- [15] S. K. Korotky, “Price-points for components of multi-core fiber communication systems in backbone optical networks,” *IEEE/OSA J. Opt. Commun. Netw.*, vol. 4, no. 5, pp. 426–435, Jun. 2012.
- [16] N. Shahriar, S. Taeb, S. R. Chowdhury, M. Tornatore, R. Boutaba, J. Mitra, and M. Hemmati, “Achieving a fully-flexible virtual network embedding in elastic optical networks,” in *Proc. Int. Conf. on Comput. Commun. (ICC)*, Paris, France, Apr. 2019, pp. 1756–1764.
- [17] S. J. Savory, “Approximations for the nonlinear self-channel interference of channels with rectangular spectra,” *IEEE Photon. Technol. Lett.*, vol. 25, no. 10, pp. 961–964, Apr. 2013.
- [18] Y. Li, H. Dai, G. Shen, and S. K. Bose, “Adaptive FEC-based lightpath routing and wavelength assignment in WDM optical networks,” *Opt. Switching Netw.*, vol. 14, pp. 241–249, Aug. 2014.
- [19] T. Koike-Akino, K. Kojima, D. S. Millar, K. Parsons, T. Yoshida, and T. Sugihara, “Pareto optimization of adaptive modulation and coding set in nonlinear fiber-optic systems,” *IEEE/OSA J. Lightw. Technol.*, vol. 35, no. 4, pp. 1041–1049, Feb. 2017.
- [20] K. Christodoulopoulos, C. Delezoide, N. Sambo, A. Kretsis, I. Sartezakis, A. Sgambelluri, N. Argyris, G. Kanakis, P. Giardina, G. Bernini *et al.*, “Toward efficient, reliable, and autonomous optical networks: the orchestra solution,” *IEEE/OSA J. Opt. Commun. Netw.*, vol. 11, no. 9, pp. C10–C24, 2019.
- [21] S. Behera, A. Deb, G. Das, and B. Mukherjee, “Impairment aware routing, bit loading, and spectrum allocation in elastic optical networks,” *IEEE/OSA J. Lightw. Technol.*, vol. 37, no. 13, pp. 3009–3020, Apr. 2019.
- [22] K. Christodoulopoulos, K. Manousakis, and E. Varvarigos, “Offline routing and wavelength assignment in transparent WDM networks,” *IEEE/ACM Trans. Netw.*, vol. 18, no. 5, pp. 1557–1570, Oct. 2010.
- [23] P. Sayyad Khodashenas, J. M. Rivas-Moscoso, B. Shariati, D. M. Marom, D. Klonidis, and I. Tomkos, “Investigation of spectrum granularity for performance optimization of flexible Nyquist-WDM-based optical networks,” *IEEE/OSA J. Lightwave Technol.*, vol. 33, no. 23, pp. 4767–4774, Dec. 2015.
- [24] D. M. Marom, P. D. Colbourne, A. Dérico, N. K. Fontaine, Y. Ikuma, R. Proietti, L. Zong, J. M. Rivas-Moscoso, and I. Tomkos, “Survey of photonic switching architectures and technologies in support of spatially and spectrally flexible optical networking [invited],” *IEEE/OSA J. Opt. Commun. Netw.*, vol. 9, no. 1, pp. 1–26, Jan. 2017.
- [25] G. Shen, Y. Zhang, X. Zhou, Y. Sheng, N. Deng, Y. Ma, and A. Lord, “Ultra-dense wavelength switched network: a special EON paradigm for metro optical networks,” *IEEE Commun. Mag.*, vol. 56, no. 2, pp. 189–195, Feb. 2018.
- [26] Yueqian. Channel capacity with QAM inputs. (Date last accessed 15-June-2020). [Online]. Available: <https://fr.mathworks.com/matlabcentral/fileexchange/31158-channel-capacity-with-qam-inputs>
- [27] P. Poggiolini, “The GN model of non-linear propagation in uncompensated coherent optical systems,” *IEEE/OSA J. Lightw. Technol.*, vol. 30, no. 24, pp. 3857–3879, Dec. 2012.
- [28] P. Johannesson and E. Agrell, “Modeling of nonlinear signal distortion in fiber-optic networks,” *IEEE/OSA J. Lightw. Technol.*, vol. 32, no. 23, pp. 3942–3950, Oct. 2014.
- [29] P. Poggiolini, G. Bosco, A. Carena, V. Curri, Y. Jiang, and F. Forghieri, “The GN-model of fiber non-linear propagation and its applications,” *IEEE/OSA J. Lightw. Technol.*, vol. 32, no. 4, pp. 694–721, Feb. 2014.
- [30] G. Zervas, E. Hugues-Salas, T. Polity, S. Frigerio, and K.-I. Sato, *Node Architectures for Elastic and Flexible Optical Networks*. Cham: Springer Int. Publishing, 2016, pp. 117–157.
- [31] Y. Pointurier, “Design of low-margin optical networks,” *IEEE/OSA J. Opt. Commun. Netw.*, vol. 9, no. 1, pp. A9–A17, Jan. 2017.
- [32] A. Magnani and S. P. Boyd, “Convex piecewise-linear fitting,” *Optimization and Engineering*, vol. 10, no. 1, pp. 1–17, Mar. 2009.
- [33] J. Y. Yen, “Finding the k shortest loopless paths in a network,” *Manag. Sci.*, vol. 17, no. 11, pp. 712–716, Jul. 1971.
- [34] J. Zhao, H. Wymeersch, and E. Agrell, “Nonlinear impairment-aware static resource allocation in elastic optical networks,” *IEEE/OSA J. Lightw. Technol.*, vol. 33, no. 22, pp. 4554–4564, Aug. 2015.
- [35] M. Ju, F. Zhou, Z. Zhu, and S. Xiao, “Distance-adaptive, low CAPEX cost p -cycle design without candidate cycle enumeration in mixed-line-rate optical networks,” *IEEE/OSA J. Lightwave Technol.*, vol. 34, no. 11, pp. 2663–2676, Apr. 2016.
- [36] P. Poggiolini, G. Bosco, A. Carena, R. Cigliutti, V. Curri, F. Forghieri, R. Pastorelli, and S. Piciaccia, “The LOGON strategy for low-complexity control plane implementation in new-generation flexible networks,” in *Proc. Opt. Fiber Commun. Conf. (OFC)*, 2013, p. OW1H.3.
- [37] F. Zhou, J. Liu, G. Simon, and R. Boutaba, “Joint optimization for the delivery of multiple video channels in Telco-CDNs,” *IEEE Trans. Netw. Service Manage.*, vol. 12, no. 1, pp. 87–100, Mar. 2015.